Coexistence of ferro- and antiferromagnetic interactions in a metal–organic radical-based (6,3)-helical network with large channels†

Daniel Maspoch,[a] Neus Domingo,[b] Daniel Ruiz-Molina,*[a] Klaus Wurst,[c] Joan-Manel Hernández,[b] Gavin Vaughan,[d] Concepció Rovira,[a] Francesc Lloret,[e] Javier Tejada[b] and Jaume Veciana*[a]

Received (in Cambridge, UK) 27th April 2005, Accepted 30th August 2005
First published as an Advance Article on the web 26th September 2005
DOI: 10.1039/b505827a

A metal–organic open-framework with an unprecedented (6,3)-helical topology, large channels and mixed ferro- and antiferromagnetic interactions has been synthesized using a three-connecting tricarboxylic polychlorotriphenylmethyl radical and Co(II) ions.

Rapid development in the self-assembly of transition metal ions and multitopic organic ligands has yielded a wide variety of one-, two- and three-dimensional metal–organic architectures that have specific properties.[1] For instance, in the field of porous metal–organic materials, the endless versatility of molecular chemistry to design new polytopic ligands has become an excellent tool to obtain open-framework structures[2] with different topologies[3] and surprising porosity properties.[4] Furthermore, along with the typical applications of porous solids as molecular sieves, sensors, ion-exchangers and catalysts, the recent construction of open-frameworks from paramagnetic transition metal ions also opens the possibility to design porous materials with additional electrical,[5] optical[6] or magnetic properties. Among them, attainment of magnetic metal–organic porous solids has attracted considerable efforts in the last few years because of their potential applications as magnetic sensors and/or low-density magnetic materials.[7,8]

So far, different polytopic ligands that allow not only control of pore sizes but also favour magnetic exchange interactions have been used.[7] In our group, we recently described a new strategy for the preparation of nanoporous materials with enhanced magnetic properties consisting of the use of purely organic radicals as "spacer" paramagnetic ligands.[9] Thus, we designed and synthesized a polytopic open-shell perchlorinated triphenylmethyl radical with three carboxylic groups (PTMTC, Fig. 1a).[10] In terms of topology, PTMTC is a trigonal bridging ligand that can be considered an expanded version of the well-known trimesic acid. Moreover, the presence of a rigid structure with bulky chlorine atoms, in addition to providing high thermal and chemical stability, would prevent interpenetration phenomena.[11] Finally, it was expected that radicals may interact magnetically with the coordinated transition metal ions enhancing the magnetic dimensionality of the porous material, in comparison with those obtained from diamagnetic polytopic ligands, as occur in metal–organic complexes with nitroxide radicals.[12] The success of this approach was initially demonstrated by the preparation of a Cu(II) (6,3)-honeycomb porous molecular sponge-like magnet (MOROF-1)[8] and a Co(II) nanoporous network with an unprecedented $(6^3)\cdot(6^9.8^1)$ topology (MOROF-2).[13]

In a further step, herein we report a new metal–organic radical open-framework material, named as MOROF-3, $[Co_6(PTMTC)_4(py)_{17}(H_2O)_4(EtOH)]$ formed by the self-assembly of 3-connected bridging PTMTC radicals and a transition metal ion with large magnetic anisotropy like Co(II). This is, to our knowledge, the first example of a nanochannel-like structure that in addition to exhibiting an unusual (6,3)-helical coordination network shows mixed ferro- and antiferromagnetic interactions between the Co(II) ions and PTMTC radicals.

Red needle-like crystals of MOROF-3 were obtained by slow diffusion of an ethanol solution of pyridine onto a solution of $Co(ClO_4)_2\cdot 6H_2O$ and PTMTC in ethanol and water.‡ Single-crystal X-ray analysis of MOROF-3 reveals a three-dimensional framework built from seven different crystallographic octahedral Co(II) units, which slightly differ in their coordination sphere (Fig. 1b).§ Indeed, although each Co(II) unit is coordinated by two PTMTC radicals, variations on the coordination mode of the

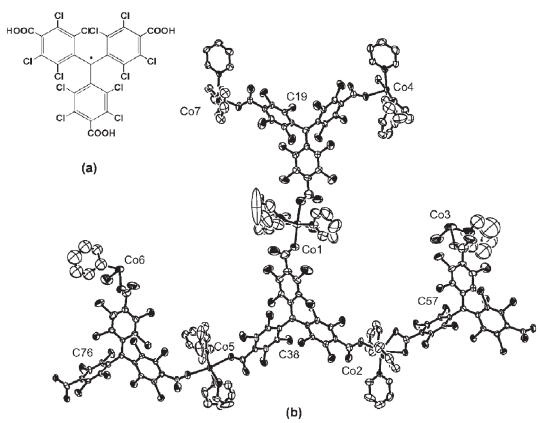

Fig. 1 a) PTMTC radical. b) ORTEP view of the asymmetric unit of MOROF-3 at 30% probability level. All H atoms are omitted for clarity.

[a]*Institut de Ciència de Materials de Barcelona (CSIC), Campus Universitari, Bellaterra, 08193, Catalonia, Spain. E-mail: vecianaj@icmab.es; Fax: 34 93 5805729; Tel: 34 93 580 1853*
[b]*Facultad de Física, Universitat de Barcelona, Diagonal 647, 08028-Barcelona, Spain*
[c]*Institut für Allgemeine Anorganische und Theoretische Chemie, Universität Innsbruck, A-6020, Innrain 52a, Austria*
[d]*European Synchrotron Radiation Facility (E. S. R. F.), B. P. 220, F-38043 Grenoble cedex, France*
[e]*Departament de Química Inorgànica, Facultat de Química de la Universitat de València, Dr. Moliner 50, E-46100 Burjasot, València, Spain*

† Electronic supplementary information (ESI) available: FT-IR, desorption characterization, shortest circuit of the (6,3)-helical network image and detailed magnetic characterization and images. See http://dx.doi.org/10.1039/b505827a

carboxylates and nature of counter-ligands are found. Two carboxylate groups of two different PTMTC moieties coordinate to Co(II) ions in a bidentate mode, whereas each of the other carboxylate groups coordinates Co(II) ions in a monodentate fashion. Two or three pyridine molecules and two or one water or ethanol molecules occupy the remaining positions on the metal centers.

An examination of the connectivity of the extended architecture of MOROF-3 shows that the shortest circuit contains six PTMTC radicals and six Co(II) atoms (see Fig. 1S of ESI). Thus, the network can be classified as a (6,3)-helical net, if the Co(II) ions are considered spacers and the moieties of PTMTC 3-connecting nodes. To better understand the structural conformation of such a pseudo "3-D" (6,3)-helical network (with one finite direction), a comparison with a representative 2-D (6,3)-honeycomb network is recommended. In principle, the (6,3)-helical network can be created from a 2-D honeycomb network by converting four of six planar sides of each hexagon to angular nodes with the appropriate orientation to bend each plane in a zigzag form, as shown in Fig. 2.

This is indeed the unusual topological situation that takes place in MOROF-3. The angles between trigonal nodes (associated with the central methyl carbons [C(19), C(38), C(57) and C(76)] of each PTMTC radical and four of six Co(II) ions [Co(2), Co(4), Co(5) and Co(7)]) range from 130 to 141°, which differ considerably from the angle of 180° required for the formation of pure 2-D honeycomb layers. Accordingly, these Co(II) ions act as angular twofold nodes to originate 1-D zigzag-type folds along each honeycomb layer, generating the (6,3)-helical network exhibited by MOROF-3. The helical nature is also favored by the propeller-shape conformation of PTMTC radicals that provides torsion angles of 45 to 56° between the mean planes of the three polychlorinated aromatic rings and the reference plane, formed by the three bridgehead C atoms and the methyl one. Thus, this arrangement can be regarded as a non-chiral helical network, growing in a pseudo-hexagonal topology along the [100] direction (Fig. 3a and b). Each helical strand is composed of four Co(II) units per turn with a pitch of 9 Å and a distance of 22–24 Å between opposite Co(II) units. This leads to the formation of non-interpenetrated 1-D nanochannels with minimum dimensions of

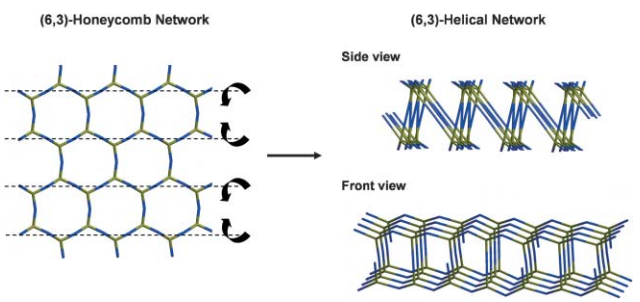

Fig. 2 Ideal generation of the (6,3)-helical network from the (6,3)-honeycomb planar network. Left: A schematic representation of the modification (denoted by the arrows) of the four angles (from 180° to 120–150°) between the trigonal nodes (green) and the metal ions (blue), required to form the zigzag-type folds along one direction of the (6,3)-honeycomb plane, in order to form the (6,3)-helical network. Right: Side and front views of the resulting (6,3)-helical network, exhibited by MOROF-3.

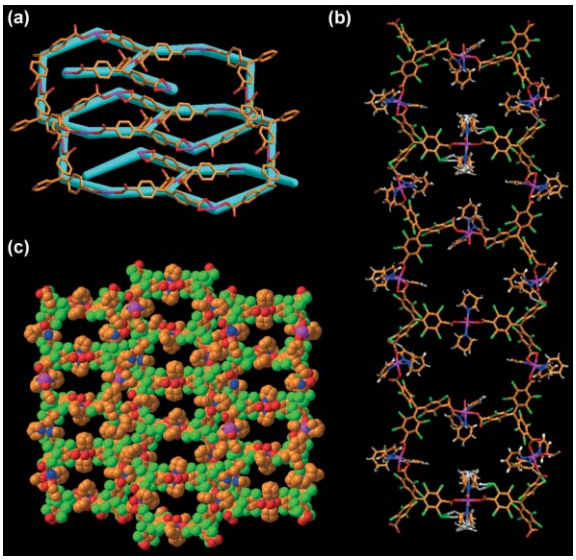

Fig. 3 Crystal structure of MOROF-3. a) Adjacent infinite helices viewed along [0½½]. Note the opposite handedness of the adjacent helices, which build the non-chiral (6,3) net. b) Illustration of the (6,3) net viewed along [100]. c) Space-filling representation of the crystal packing of (6,3) nets viewed along [100], showing the nanochannels. Co, purple; C, orange-brown; O, red; Cl, green; N, blue; H, white.

17.5 × 6.8 Å when van der Waals radii are considered (Fig. 3c). The resulting cavities are large enough to endow this material with a total void volume of 38% of the cell volume. In absolute terms, it represents a volume of 5492 $Å^3$ per 14412 $Å^3$ of the unit cell. Such a volume is occupied by disordered ethanol and water solvent molecules that can be evacuated. The overall structure thus formed could be regarded as the packing of individual channel-like (6,3) nets along the [011] direction. The infinite nets are stacked with a (0,b/4,c/4) displacement and connected by noncovalent interactions such as non-classical H-bonds, face-to-face π–π interactions and Cl–Cl contacts.

The thermal variation of magnetic susceptibility for a crystalline as-synthesized sample of MOROF-3 was measured on a SQUID magnetometer in the temperature range of 1.8–300 K, under external applied magnetic fields of 0.1 to 10 kG. The inset of Fig. 4 shows the temperature dependence of the product of molar magnetic susceptibility with temperature ($\chi_m \cdot T$). The value of 22 $cm^3 \cdot K \cdot mol^{-1}$ at room temperature differs from the expected spin-only value of 12.75 $cm^3 \cdot K \cdot mol^{-1}$ calculated for six Co(II) ions and four PTMTC radicals with $g = 2$ and local spins $S_{Co} = 3/2$ and $S_{PTMTC} = 1/2$, respectively, indicating a large magnetic orbital contribution of the six-coordinating Co(II) ions. Upon lowering the temperature, $\chi_m \cdot T$ smoothly decreases until it reaches a minimum value of 13.7 $cm^3 \cdot K \cdot mol^{-1}$ around 16 K. This decrease is related to the depopulation of the higher energy Kramer's doublets of the Co(II) centers with a $^4T_1$ term as the ground state. In fact, this magnetic behaviour can be theoretically modeled in the temperature range of 30–300 K, as a non-interacting system of six octahedral Co(II) ions with strong spin–orbit coupling and four magnetically isotropic PTMTC radicals.

The Hamiltonian describing the Co(II) ions is given by Eq. 1,

$$\mathscr{H} = -Ak\lambda \mathrm{LS} + D[L_z^2 - 1/3(L(L+1))] + \beta(-Ak\mathrm{L} + g_e\mathrm{S})H \quad (1)$$

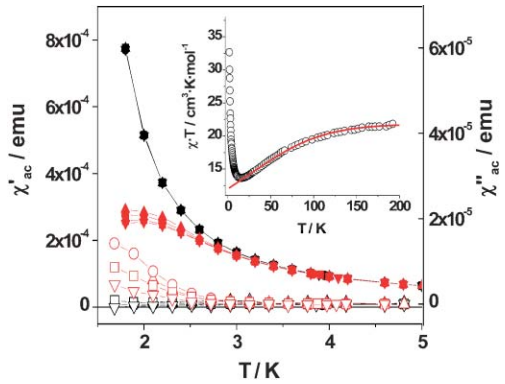

Fig. 4 AC magnetic susceptibility measurements as a function of the temperature at H_{ac} = 3.8 Oe at different frequencies for H_{dc} = 0 G (black) and H_{dc} = 500 G (red): (▼) 300 Hz, (■) 30 Hz, (●) 3 Hz, (▲) 0.3 Hz. Full and empty symbols stand for in-phase and out-of-phase components, respectively. The inset shows the experimental and calculated $\chi_m \cdot T$ as a function of the temperature for the as-synthesized MOROF-3 at H = 1000 G. The theoretical curve is calculated with the parameters given in the text for the case of D = 0 cm^{-1}.

from where using matrix diagonalization techniques we obtained the following values for the parameter A = 1.47(1) (factor due to T–P isomorphism), λ = −110(5) cm^{-1} (spin–orbit coupling parameter), k = 0.96(2) (orbital reduction parameter), and $-100 < D < +100$ cm^{-1} (see ESI).[14] Given that these parameters are able to reproduce the experimental data for temperatures over 30 K (inset Fig. 4), no significant magnetic coupling between magnetic centres is expected above this temperature. However, below 16 K, the $\chi_m \cdot T$ value increases rapidly up to a value of 32.7 $cm^3 \cdot K \cdot mol^{-1}$ at 1.8 K, similarly as in other examples.[15] This abrupt increase is probably due to an increase of the correlation length of ferromagnetically-coupled units as randomising thermal effects are reduced, most likely *via* an in-helical (6,3) net long-range magnetic ordering. Moreover, such a maximum becomes field dependent (see Fig. 2S of ESI) as an effect of the saturation of the magnetization.

The field-dependent magnetization curve at 1.8 K (see Fig. 3S of ESI) rapidly increases up to a value of 12.2 μB at 5 T, although a complete saturation is not reached at this applied magnetic field. For a six-coordinated Co(II) ion at very low temperature, only the ground state of the Kramer's doublet is populated. An effective spin S_{eff} = 1/2 with a $g = (10 + 2Ak)/3$ can be associated with this Kramer's doublet. So, the saturation value of the magnetization, Ms, for a Co(II) ion is Ms = Nμβ/2, in our case Ms *ca.* 2.1 μβ (for A = 1.47 and k = 0.96). The corresponding value for a radical (g = 2 and S = 1/2) is *ca.* 1 μβ. In this sense, if all magnetic interactions were ferromagnetic, a value of Ms *ca.* 16.6 μβ, for six Co(II) ions and four radicals (6 × 2.1 + 4 × 1), would be expected. However, in the case where the magnetic interactions were antiferromagnetic, a value of Ms *ca.* 8.6 μβ (6 × 2.1 − 4 × 1) would be expected. Due to the fact that Ms of MOROF-3 has an intermediate value between the above two cases, the coexistence of ferro- and antiferromagnetic interactions most likely occurs. This is possible because of the different coordination modes (bidentate and monodentate) of the radicals with Co(II) ions, and the different angles between the trigonal nodes.

No evidence of a hysteresis loop was observed at 1.8 K although an incipient out-of-phase signal of the ac magnetic susceptibility, χ_m'', under an external magnetic field, appears below 3 K. When a dc magnetic field greater than 500 G is applied, both components of ac susceptibility show weak frequency dependent peaks over a range of 0.3–300 Hz (Fig. 4), suggesting that a bulk magnetic order could occur below 1.8 K.

In summary, MOROF-3 exhibits an unusual (6,3)-helical structure which is closely related to the typical (6,3)-honeycomb observed in MOROF-1.[9] This new architecture confirms the huge coordinating versatility and ability of this open-shell ligand to build nanostructured networks with combined large pores and empty volumes. Furthermore, this is the first time that ferromagnetic exchange interactions between polychlorotriphenylmethyl radicals and metal Co(II) ions have been detected.

This work was supported by the DGI (Spain), under project MAT2003-04699, and by the European Community under the Marie Curie Research Training Network (contract "QUEMOLNA", number MRTN-CT-2003-504880). We also thank the ESRF for providing time (CH-1236) on the ID-11 beam line.

Notes and references

‡ Slow diffusion (28 days) of a solution of pyridine (0.5 mL) in ethanol (2 mL) onto a solution of $Co(ClO_4)_2 \cdot 6H_2O$ (0.0684 mmol) and PTMTC (0.0456 mmol) in ethanol (1.6 mL) and water (0.4 mL) yielded red needle crystals of MOROF-3.

§ *Crystal data* for MOROF-3: $C_{175}H_{99}Cl_{48}Co_6N_{17}O_{29} \times 2\ H_2O \times 4$ EtOH triclinic, space group *P*-1, a = 9.0119(9), b = 34.547(7), c = 46.453 (9) Å, α = 89.623(4), β = 85.250(9), γ = 89.862(11)°, vol = 14412(4), Z = 2, D_c = 1.193 g cm^{-3}, μ = 0.431 mm^{-1}, $F(000)$ = 5204, T = 293(2) K, $-8 \leqslant h \leqslant 8$, $-34 \leqslant k \leqslant 34$, $-46 \leqslant l \leqslant 46$. Final results (for 2501 parameters) were R_1 = 0.1077 and wR_2 = 0.2922 for 18173 reflections with $I > 2\sigma(I)$. CCDC 260718. See http://dx.doi.org/10.1039/b505827a for crystallographic data in CIF or other electronic format.

1 C. Janiak, *Dalton Trans.*, 2003, 2781.
2 (*a*) O. M. Yaghi, M. O'Keeffe, N. W. Ockwig, H. K. Chae, M. Eddaoudi and J. Kim, *Nature*, 2003, **423**, 705; (*b*) R. Robson, *J. Chem. Soc., Dalton Trans.*, 2000, 3735; (*c*) A. J. Blake, N. R. Champness, P. Hubberstey, M. Schröder and M. A. Withersby, *Coord. Chem. Rev.*, 1999, **183**, 117.
3 B. Moulton and M. J. Zaworotko, *Chem. Rev.*, 2001, **101**, 1629.
4 S. Kitagawa, R. Kitaura and S. Noro, *Angew. Chem., Int. Ed.*, 2004, **43**, 2334 and references cited therein.
5 G. J. Halder, C. J. Kepert, B. Moubaraki, K. S. Murray and J. D. Cashion, *Science*, 2002, **298**, 1762.
6 G. Seward, W.-L. Jia, R.-Y. Wang, G. D. Enright and S. Wang, *Angew. Chem., Int. Ed.*, 2004, **43**, 2933.
7 D. Maspoch, D. Ruiz-Molina and J. Veciana, *J. Mater. Chem.*, 2004, **14**, 2713 and references cited therein.
8 O. Kahn, J. Larionova and J. V. Yakhmi, *Chem. Eur. J.*, 1999, **5**, 3443.
9 D. Maspoch, D. Ruiz-Molina, K. Wurst, N. Domingo, M. Cavallini, F. Biscarini, J. Tejada, C. Rovira and J. Veciana, *Nat. Mater.*, 2003, **2**, 190.
10 D. Maspoch, N. Domingo, D. Ruiz-Molina, G. Vaughan, K. Wurst, J. Tejada, C. Rovira and J. Veciana, *Angew. Chem., Int. Ed.*, 2004, **43**, 1828.
11 K. Kobayashi, T. Shirasaka, A. Sato, E. Horst and N. Furukawa, *Angew. Chem., Int. Ed.*, 1999, **38**, 3483.
12 (*a*) A. Caneschi, D. Gatteschi and P. Rey, *Prog. Inorg. Chem.*, 1991, **39**, 331; (*b*) H. Iwamura, K. Inoue and T. Hayamizu, *Pure Appl. Chem.*, 1996, **68**, 243.
13 D. Maspoch, D. Ruiz-Molina, K. Wurst, C. Rovira and J. Veciana, *Chem. Commun.*, 2004, 1164.
14 B. N. Figgis, M. Gerloch, J. Lewis, F. E. Mabbs and G. A. Webb, *J. Chem. Soc., A*, 1968, 2086.
15 F. Lloret, G. Demunno, M. Julve, J. Cano and A. Caneschi, *Angew. Chem., Int. Ed.*, 1998, **37**, 135.